

Contact inhibition of locomotion *in vivo* controls neural crest directional migration

Carlos Carmona-Fontaine¹, Helen K. Matthews¹, Sei Kuriyama¹, Mauricio Moreno¹, Graham A. Dunn², Maddy Parsons², Claudio D. Stern¹ & Roberto Mayor¹

Contact inhibition of locomotion was discovered by Abercrombie more than 50 years ago and describes the behaviour of fibroblast cells confronting each other *in vitro*, where they retract their protrusions and change direction on contact^{1,2}. Its failure was suggested to contribute to malignant invasion^{3–6}. However, the molecular basis of contact inhibition of locomotion and whether it also occurs *in vivo* are still unknown. Here we show that neural crest cells, a highly migratory and multipotent embryonic cell population, whose behaviour has been likened to malignant invasion^{6–8}, demonstrate contact inhibition of locomotion both *in vivo* and *in vitro*, and that this accounts for their directional migration. When two migrating neural crest cells meet, they stop, collapse their protrusions and change direction. In contrast, when a neural crest cell meets another cell type, it fails to display contact inhibition of locomotion; instead, it invades the other tissue, in the same manner as metastatic cancer cells^{3,5,9}. We show that inhibition of non-canonical Wnt signalling abolishes both contact inhibition of locomotion and the directionality of neural crest migration. Wnt-signalling members localize at the site of cell contact, leading to activation of RhoA in this region. These results provide the first example of contact inhibition of locomotion *in vivo*, provide an explanation for coherent directional migration of groups of cells and establish a previously unknown role for non-canonical Wnt signalling.

Neural crest (NC) cells cultured *in vitro* move away from each other, dispersing quickly¹⁰. *Xenopus* NC explants revealed that only the leading-edge cells were polarized, having large lamellipodia at the front as shown by scanning electron microscopy (arrowheads in Fig. 1a–c) or in a live NC explant expressing membrane-localized green fluorescent protein (GFP) (Fig. 1d). Time-lapse analysis revealed that edge cells had a higher persistence in the direction of migration than cells in the interior of the explant (Fig. 1d'). To establish whether these differences in polarity and migration correspond to two different cell populations or whether they are due to cell–cell contact, we dissociated NC explants into single cells and then re-aggregated them into small or large clusters. Peripheral cells in small or large clusters rapidly became polarized and migrate away from each other (Fig. 1e), whereas internal cells moved randomly (Supplementary Fig. 2 and Supplementary Movie 1), similarly to those in non-dissociated explants. In addition, the randomly migrating internal cells of these explants became polarized when made to have a free edge by wounding or removal of their neighbours (Supplementary Fig. 3). These results suggest that the differential behaviour of leading versus internal cells in explants is due not to intrinsic cell differences but to interactions between neighbouring cells. Furthermore, the average persistence of the leading cells (defined by their position at the border of an explant) in a

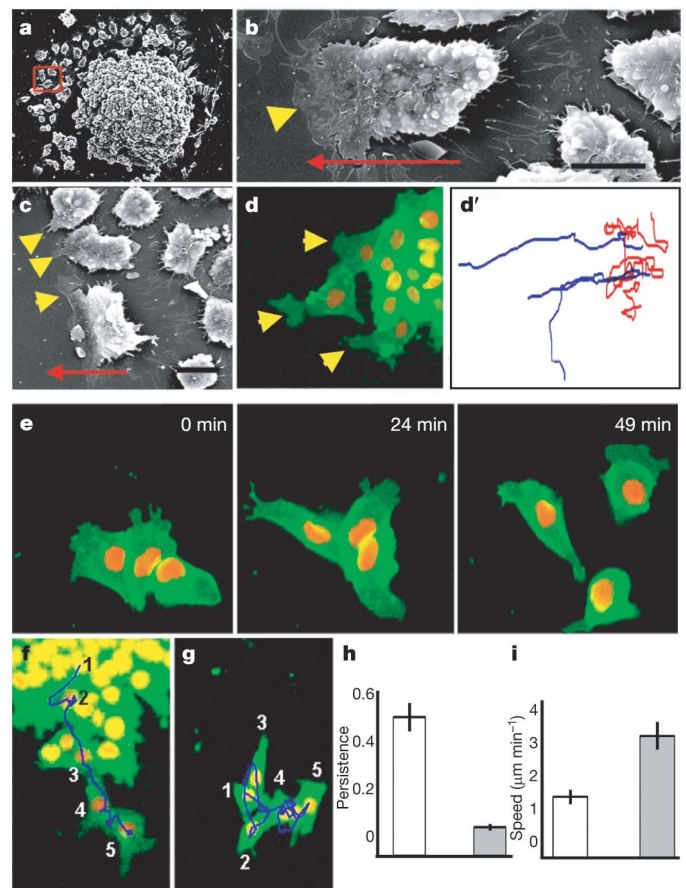


Figure 1 | Cell-cell contacts polarize migrating NC cells *in vitro*. a–g, NCs were cultured *in vitro* and analysed by scanning electron microscopy (a–c) or time-lapse microscopy of cells expressing membrane-GFP and nuclear-RFP (d–g). The red square in a indicates leading cells (defined by its position at the edge of migration); higher magnifications of other leading cells are shown in b and c. Arrowheads indicate lamellipodia (note their presence only in the leading cells, either by scanning electron microscopy (c); or fluorescence (d)); the arrow indicates the direction of migration. Scale bars in b, c, 50 μm . d', Tracks of leading (blue) and trailing (red) cells shown in d. e, Three frames of a time-lapse movie for dissociated and re-aggregated NC cells. f, g, Temporal projection to compare the migration of a group of NC cells (f) with that of individual cells (g). Numbers indicate the position of the same cell at different time frames 10 min apart. The track is shown as a blue line. h, i, Persistence (h) and speed of migration (i) for the migration as a group (white bars) or as an individual cell (grey bars) ($P < 0.005$, $n = 60$). Error bars show s.d.

¹Department of Anatomy and Developmental Biology, University College London, London WC1E 6BT, UK. ²Randall Division of Cell and Molecular Biophysics, King's College London, London SE1 1UL, UK.

non-dissociated cluster was much higher than that of individual cells; the latter often made little progress and moved in circles, although their overall speed of migration was greater (Fig. 1f–i and Supplementary Movie 2). A similar phenomenon has been reported for cell types showing contact inhibition of locomotion¹. Taken together, these results indicate that the directional migration of cultured NC cells is dependent on cell–cell contact, which is likely to inhibit the formation of cell protrusions, leading to cell polarization.

To study the behaviour of NC cells when confronted with other cells, we developed an explant-confrontation assay^{1,11}. Two NC explants were cultured in close proximity such that their leading cells would encounter cells from the other explant migrating in the opposite direction (Fig. 2A). We found that cells from NC explants aggressively invaded mesodermal (Fig. 2E) and ectodermal (not shown) explants, but never invaded other NC explants (Fig. 2C, Supplementary Fig. 4a–c and Supplementary Movie 3). Confocal microscopic analyses showed that whereas NC cells stopped migrating when confronted with other NC cells, they engulfed the mesoderm explant, with some cells penetrating deep layers of this tissue (Fig. 2D, F and Supplementary Fig. 4d–i). These observations suggest

that contact inhibition of locomotion occurs between NC cells (homotypic) but not between NC cells and other cell types (heterotypic), in the same way as with some malignant cells^{4,5,9}.

It is tempting to speculate that such homotypic contact inhibition of locomotion could function in guiding the migration of NC cells in normal development. To determine whether this is true we developed a confrontation assay *in vivo* and found that NC cells can invade the tissue of an adjacent *Xenopus* embryo lacking NC (Fig. 2O) but this invasion is blocked when the host NC is present (Fig. 2N). This result is compatible with contact inhibition of locomotion having this function, but it does not directly demonstrate that NC cells show contact inhibition of locomotion. We therefore performed time-lapse analysis in the explant-confrontation assay, focusing on individual cells. When a NC cell came into contact with a cell from the opposite group, its lamellipodium collapsed and the direction of its migration changed (Fig. 2G and Supplementary Movie 4). This is described precisely by Abercrombie's original definition of contact inhibition of locomotion as "the phenomenon of a cell ceasing to continue moving in the same direction after contact with another cell"⁵. So far, contact inhibition of locomotion has been

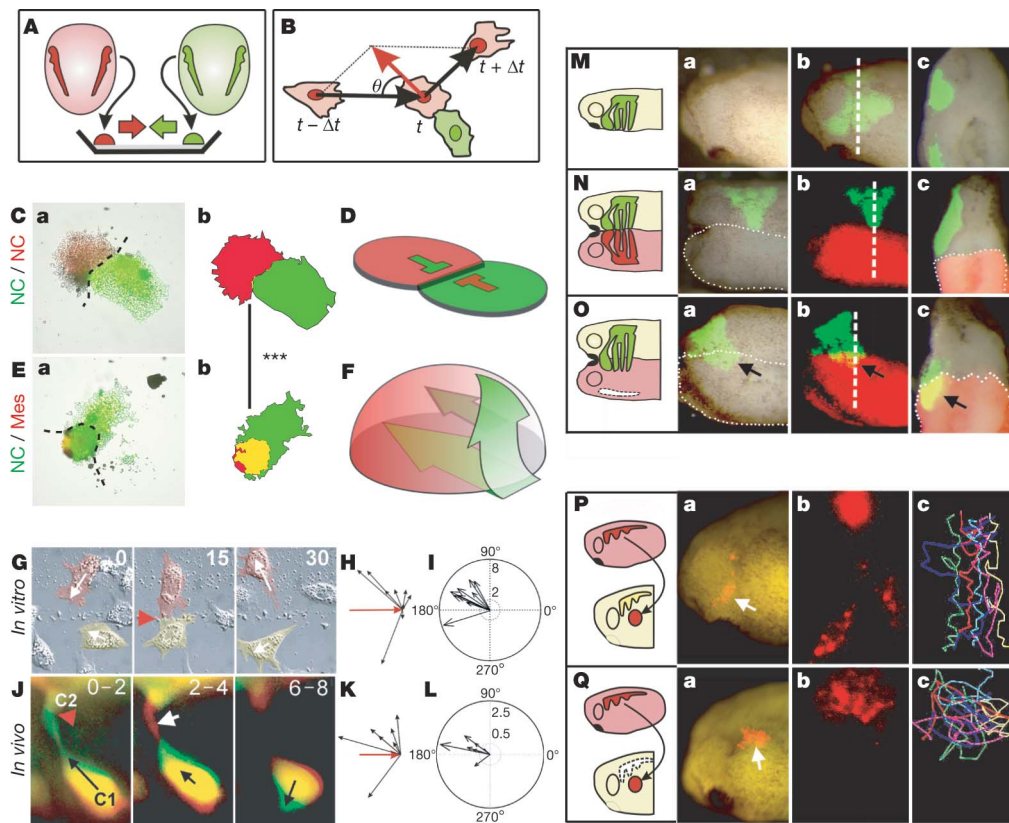


Figure 2 | Contact inhibition of locomotion in NC cells *in vitro* and *in vivo*.

A, Experimental design. **B**, Analysis of contact inhibition of locomotion. Mean velocities were measured Δt minutes before and after the collision. Acceleration (red) was calculated for each cell. The angle of collision, θ , was calculated after initial trajectory alignment. **C–F**, Invasion of confronted explants *in vitro*. **C**, There is no invasion in NC/NC confrontations (**a**), outlines in (**b**), overlapping area in yellow; shown schematically in **D**. **E**, NC explants completely invade and cover mesodermal (mes) explants (**a**), outlines in (**b**), overlapping area in yellow; shown schematically in **F**. Green arrows in **F** indicate the NC path of invasion (see Supplementary Fig. 3 for supporting confocal images). Three asterisks in **b** show a significant difference in the overlapping area (yellow), $P < 0.005$ ($n = 5$ for each condition). **G–L**, Contact inhibition of locomotion. **G**, Collision between two pseudocoloured NC cells *in vitro*. Time is shown in minutes. White arrows indicate the direction of migration; the red arrowhead indicates collision. **H**, Velocity vectors for NC *in vitro*; the red arrow indicates the initial velocity vector. **I**, Acceleration vectors for NC collisions *in vitro*. They are clustered

after the collision ($P < 0.005$, $n = 10$). **J**, Collision of two NC cells (C1 and C2) *in vivo* shown as the difference between two consecutive 2-min frames. Green, new area; red, collapsing area; black arrow, direction of migration; red arrowhead, cell contact; white arrow, collapsing protrusion. **K**, *In vivo* velocity vectors. **L**, *In vivo* acceleration. They are clustered after the collision ($P < 0.01$, $n = 10$). **M–O**, NC invasion *in vivo*. **a**, **b**, lateral view; **c**, transverse section along the dashed line shown in **b**. **M**, Labeled and transplanted NC cells in control embryos migrate normally. **N**, **O**, NC cells are not able to invade an adjacent embryo that has NC (**N**; 0% of invasion, $n = 15$), but they can invade an embryo without NC (**O**; arrow, 80% of invasion, $n = 10$). **P**, **Q**, Cell directionality *in vivo*. A small group of nuclear-RFP-labelled NC cells were grafted into a normal embryo (**P**) or into an embryo from which the NC had previously been removed (**Q**). Note that grafted cells migrated directionally in the intact embryo (persistence 0.6 ± 0.04 (mean \pm s.d.), $n = 30$), but not when the host NCs were removed (persistence 0.2 ± 0.02 (mean \pm s.d.), $n = 20$).

described only *in vitro*. To address whether it also occurs *in vivo*, we used two Sox10–GFP transgenic zebrafish lines, one expressing GFP in the cytoplasm¹² and the other in the membrane of NC cells, and analysed their migration using live-imaging techniques. Similarly to the observations *in vitro*, whenever two NC cells made contact, they changed their direction of migration and their protrusions collapsed (Fig. 2J, Supplementary Fig. 5 and Supplementary Movies 5–7). Contact inhibition of locomotion can be measured by the change in velocity after cell–cell contact^{4,11}. Large changes in the direction of cell migration were seen after each cell collision (Fig. 2B and Supplementary Methods) both *in vitro* and *in vivo* (velocity is shown in Fig. 2H, K, acceleration in Fig. 2I, L). The changes were not stochastic but were strongly biased in the opposite direction to the collision ($P < 0.005$), as predicted by Abercrombie^{5,11}. Similarly, in *Xenopus*, grafted NC cells integrated into the endogenous migratory pathway and migrated directionally (Fig. 2P). However, grafted NC lost their directional migratory behaviour when the host NC was removed (Fig. 2Q), suggesting that the directionality of NC migration depends on interactions with other NC cells and supporting our conclusion that contact inhibition of locomotion is required for normal NC migration *in vivo*.

We next explored the molecular mechanisms underlying contact inhibition of locomotion in NC cells. Previous studies have shown that the Wnt planar cell polarity (PCP, or non-canonical) pathway is

required for NC migration in *Xenopus* and zebrafish embryos, whereas canonical Wnt signalling is not^{13,14}. To determine whether PCP signalling is involved in contact inhibition of locomotion, we analysed cells expressing a dominant-negative form of *dishevelled* (*DshDep*⁺), which specifically inhibits the PCP pathway¹⁵. In control explants, only the leading cells were highly polarized, extending cell protrusions at the front, whereas trailing cells were not (Fig. 1a–c). In contrast, *DshDep*⁺ cells were not polarized but extended large protrusions in all directions (Fig. 3a–c). Live imaging showed that cells expressing *DshDep*⁺ crawled on top of one another, extending protrusions between the neighbour cells, a characteristic of some metastatic cancer cells^{3,5,9} (Fig. 3d, e, and Supplementary Movie 8). All *DshDep*⁺ (leading and trailing) cells behaved similarly to trailing control cells on the basis of their low persistence of migration and the angles at which they changed direction (Fig. 3f–i). No difference in persistence and speed of migration was observed between dissociated control and *DshDep*⁺ cells: both behaved like trailing cells (Fig. 3j–m and Supplementary Movie 9). This indicates that the effect of PCP signalling on NC migration requires cell–cell contact.

To test whether contact inhibition of locomotion is dependent on PCP signalling *in vivo*, we measured the speed of cell migration before and after cell collision in control embryos and in embryos in which PCP signalling had been disrupted (either by expressing *DshDep*⁺, by a dominant-negative form of the PCP ligand Wnt11 or by antisense morpholinos against the PCP pathway members *strabismus* (*Stb*; ref. 16) or *prickle1* (*Pk1*; ref. 17)). The lamellipodia of PCP-inhibited cells failed to collapse when they collide with each other *in vivo*, even after 1 h of contact (control, Supplementary Fig. 6a; PCP disrupted, Supplementary Fig. 6b, c; Supplementary Movie 10). In contrast to control cells (Fig. 4a, g), these cells did not significantly change their direction of migration (Fig. 4b–d), and as shown by the small acceleration vectors, cell velocity was hardly affected by cell–cell contact ($P \gg 0.05$; Fig. 4h–j). Rather, PCP-inhibited cells migrated on top of one another, remaining in close contact (Supplementary Movie 10). Similar observations were made *in vitro* after inhibition of PCP signalling by the expression of *DshDep*⁺, by a dominant-negative form of Wnt11 (*dnWnt11*)¹⁵, by a morpholino against a protein closely related to mammalian Wnt11 (*Wnt11R*)^{18,19} or by a mixture of *dnWnt11* and *Wnt11R* (Fig. 4e, f, k, l, and Supplementary Fig. 7e, f), where PCP inhibited cells did not collapse their protrusions after the collision (Supplementary Fig. 7a–c). Moreover, when control cells and *DshDep*⁺-expressing cells were confronted, only control cells collapsed their lamellipodia and moved away from the *DshDep*⁺ cells (Supplementary Fig. 7d and Supplementary Movie 11), indicating that PCP/Dsh signalling is required only in the responding cell.

Activation of the PCP pathway is typically accompanied by membrane localization of Dishevelled (Dsh)²⁰. We therefore analysed the subcellular localization of Dsh during NC migration *in vitro* and *in vivo*. In both premigratory NC cells and NC cells cultured on poly-(L-lysine), a non-permissive substrate for NC migration²¹, Dsh was seen in cytoplasmic dots (Supplementary Fig. 8a, b). In contrast, clear membrane localization of Dsh was observed at cell–cell contacts of NC cells grown on a permissive fibronectin substrate (Fig. 4o). For the leading cell, the region of cell–cell contact, and therefore the region of Dsh accumulation, was at the trailing end of the cell *in vitro* (Supplementary Fig. 8c). When two leading cells collided, Dsh became relocalized at the point of cell–cell contact, with a subsequent change in the direction of migration (Fig. 4p and Supplementary Movie 12). Similar observations on Dsh localization at cell–cell contacts between NC cells and at the trailing end of a leading cell were made *in vivo* (Supplementary Fig. 8e, f). A lack of PCP signalling led to a loss of Dsh accumulation in the cell contact (Supplementary Fig. 9). This membrane-localized Dsh is reminiscent of the foci described after activation of Dsh in mesodermal cells²². We also observed a redistribution of Wnt11 and the receptor Fz7 at cell–cell contacts *in vitro* (Fig. 4m, n) and *in vivo* (Supplementary Fig. 8g, and not

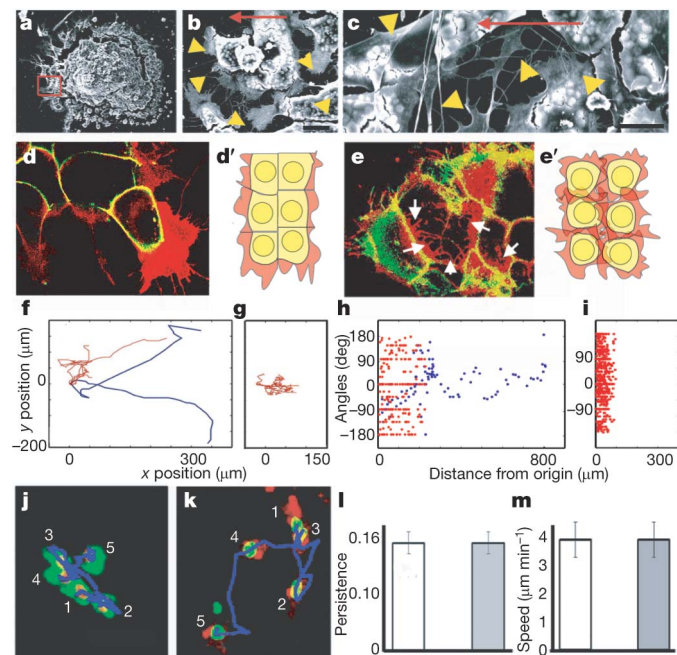


Figure 3 | Effect of PCP signalling on cell contacts. a–c, Scanning electron microscopy of *Xenopus* cultured NC expressing *DshDep*⁺. The red square indicates leading cells. Higher magnifications of other leading cells are shown in b and c. Arrowheads indicate cell protrusions; the arrow indicates the direction of migration. Scale bars, 25 μm (b), 50 μm (c). d, e, Two-plane confocal image to show cell protrusions (red) and cell shape (green). Cell protrusions are produced only at the border of the control explant (d), whereas they are observed between the *DshDep*⁺ cells (arrows in e). d', e', Schematic representations of d and e, respectively. f–i, Analysis of tracks of migrating NC cells. Blue, leading cells; red, trailing cells. f, g, Tracks of control (f) and *DshDep*⁺ (g) cells. h, i, Plots of distribution of angles of migration for leading (blue) and trailing (red) control (h) and *DshDep*⁺ (i) cells against the distance from the origin. j–m, Analysis of migration of dissociated NC cells. j, k, Five frames taken every 10 min were overlapped for a control cell (j) and a *DshDep*⁺ cell (k). Numbers indicate consecutive positions of the cell. The blue lines shows the tracks. l, m, Persistence (l) and speed of migration (m) were calculated for control (white bars) and *DshDep*⁺ (grey bars) cells ($P < 0.05$; $n = 62$). Error bars show s.d.

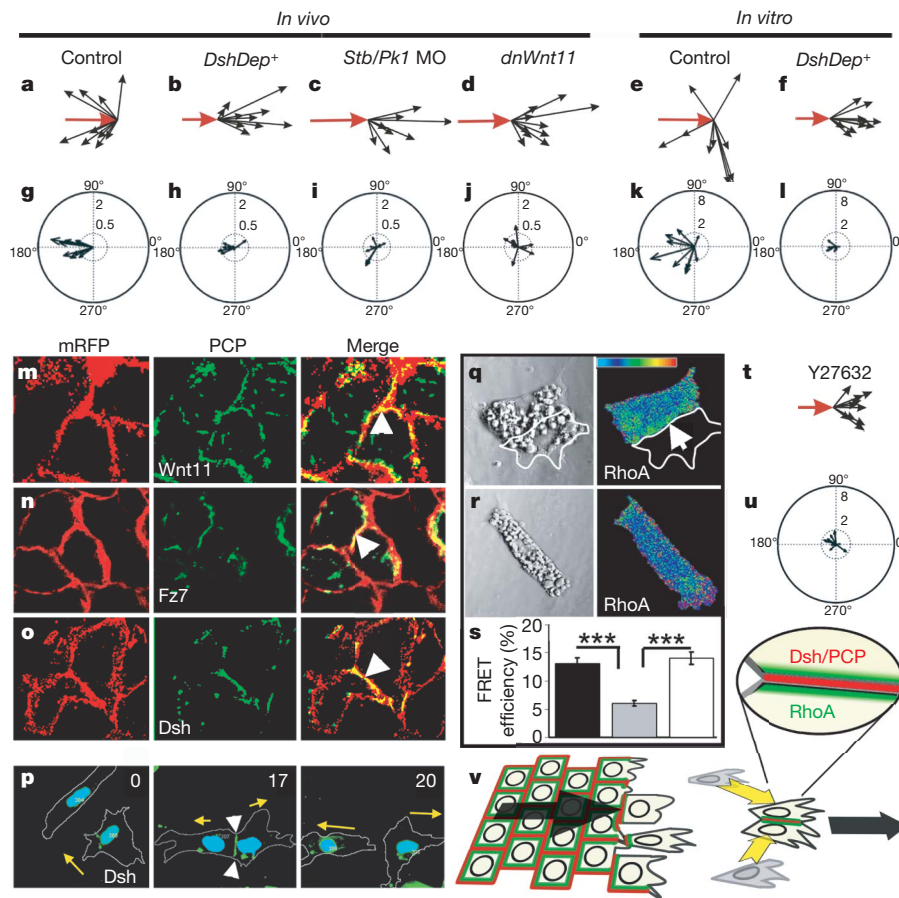


Figure 4 | Contact inhibition of locomotion: requirement of PCP and RhoA activities. **a–l**, Cell collisions were analysed *in vivo* (**a–d**, **g–j**) and *in vitro* (**e**, **f**, **k**, **l**). Velocities (**a–f**) and accelerations (**g–l**) were measured after the indicated treatments. MO, morpholino. The scales are the same for all panels. The change of velocity was significantly clustered in the controls ($P < 0.005$, $n = 10$). No significant change was observed in any of the PCP treatments ($P \gg 0.05$, $n = 10$ for all cases). **m–p**, Different PCP components are localized at the cell–cell contact (arrowheads). mRFP, membrane-RFP. **m**, Wnt11–YFP (yellow fluorescent protein). **n**, Fz7–YFP. **o**, Dsh–GFP. **p**, Cells expressing Dsh–GFP were analysed during a cell collision. The outline of the cell is taken from the differential interference contrast images. Time is shown in minutes. The arrow indicates the direction of migration;

shown); both became co-localized at the trailing end of the leading cell (Supplementary Fig. 8d). Our results suggest that cell–cell contacts polarize the cell by regulating the accumulation of ligands, receptors and intracellular element of the PCP signalling pathways.

It is well established that small GTPases are important in cell polarity and cell migration. One of them, RhoA, is a known downstream effector of PCP/Dsh during NC migration¹⁴. To examine a possible role for RhoA in contact inhibition of locomotion, we analysed the levels of RhoA activity in isolated and colliding cells by fluorescence resonance energy transfer (FRET). A significant increase in RhoA activity was detected during cell collision, with the highest activity in regions of cell–cell contact (Fig. 4q–s). When PCP signalling was activated in individual cells by expressing *DshΔN*^{13,15} a similar increase in RhoA activity was observed (Fig. 4s and Supplementary Fig. 10a–c). Finally, inhibition of Rock, a downstream target of RhoA, led to a complete loss of contact inhibition of locomotion (Fig. 4t, u, Supplementary Fig. 10d and Supplementary Movie 13). These results implicate RhoA as downstream effector of the PCP in contact inhibition of locomotion.

Although contact inhibition of locomotion was described for cultured cells more than 50 years ago^{1,2}, we present the first evidence that it occurs *in vivo* and has a key function in the directional migration of

the arrowhead indicates cell contact showing Dsh localization. **q–u**, Role of RhoA. **q–s**, FRET analysis of RhoA activity. **q**, Two NC cells in contact showing RhoA activity localized at the cell contact (arrow). **r**, Single NC cell. **s**, RhoA FRET efficiency. Black bar, cells in contact; grey bar, single cell; white bar, single cell in which PCP has been activated by the expression of *DshΔN*. Three asterisks, $P < 0.005$ ($n = 12$ for each condition). Error bars show s.d. **t**, **u**, Cell collisions were analysed in the presence of the Rock inhibitor Y27632. **t**, Velocity vectors; **u**, acceleration vectors. No significant change in velocity was observed ($P \gg 0.05$, $n = 10$). **v**, Contact inhibition of locomotion is controlled by localization of PCP elements (red) and RhoA activity (green) at the cell contact, leading to directional migration (arrows).

NC cells. We show that the PCP (non-canonical) Wnt pathway is involved in the process. The data are consistent with a model (Fig. 4v) in which cell–cell contact leads to the localized activation of the PCP signalling in the region of cell contact, which is required for the activation of RhoA. The localization of RhoA at the cell contact directs the collapse of cell protrusions and the change in cell polarity. It is commonly believed that directional cell migration during embryogenesis involves the localized production of molecules that attract migrating cells (chemotaxis)^{23–25}. Although we do not rule out chemoattraction, we suggest that contact inhibition of locomotion could be sufficient for NC directional migration. This mechanism could also direct the coherent migration of groups of cells (for example mesoderm²⁶ or lateral line primordium²⁷) and the efficient occupation by one cell population of another's territory during metastasis or development (including NC, angioblasts and neurons^{28,29}). Most cells migrating *in vivo* maintain close proximity and move in groups. Accordingly, the inhibition of cell protrusions between these clustered cells is equivalent to the process of contact inhibition of locomotion. Their typical coherent directional migration is accomplished through a 'tip-toe' movement in which front cells can move only towards the NC-free zone; that is, forwards. This opens a little space where trailing cells move, and so on (Supplementary Fig. 1).

NC cells behave similarly to some cancer cells in that they display contact inhibition of locomotion towards like, but not towards unlike, cell types^{3,5-9}. We propose that homotypic contact inhibition of locomotion confers cells with directionality during migration and that the lack of heterotypic contact inhibition allows them to invade other tissues.

METHODS SUMMARY

Xenopus NC was labelled with nuclear-red fluorescent protein (RFP)/membrane-GFP or membrane-RFP/nuclear-GFP. *In vitro* analysis of NC migration was performed with *Xenopus* NCs cultured on fibronectin-coated plates. For *in vivo* studies we used *Xenopus* embryos grafted with labelled NC or zebrafish transgenic-line embryos expressing cytoplasm or membrane-GFP under the NC promoter *sox10*. Time-lapse photography was performed with differential interference contrast or fluorescent/confocal microscopy. FRET analysis was performed as described in ref. 14. Full methods are given in Supplementary Methods.

Received 17 July; accepted 19 September 2008.

Published online 10 December 2008.

- Abercrombie, M. & Heaysman, J. E. M. Observations on the social behaviour of cells in tissue culture. I. Speed of movement of chick heart fibroblasts in relation to their mutual contacts. *Exp. Cell Res.* **5**, 111–131 (1953).
- Abercrombie, M. & Heaysman, J. E. M. Observations on the social behaviour of cells in tissue culture: II. 'Monolayering' of fibroblasts. *Exp. Cell Res.* **6**, 293–306 (1954).
- Abercrombie, M. & Heaysman, J. E. Invasiveness of sarcoma cells. *Nature* **174**, 697–698 (1954).
- Paddock, S. W. & Dunn, G. A. Analysing collisions between fibroblasts and fibrosarcoma cells: fibrosarcoma cells show an active invasive response. *J. Cell Sci.* **81**, 163–187 (1986).
- Abercrombie, M. Contact inhibition and malignancy. *Nature* **281**, 259–262 (1979).
- Hendrix, M. J. *et al.* Reprogramming metastatic tumour cells with embryonic microenvironments. *Nature Rev. Cancer* **7**, 246–255 (2007).
- Kulesa, P. M. *et al.* Reprogramming metastatic melanoma cells to assume a neural crest cell-like phenotype in an embryonic microenvironment. *Proc. Natl Acad. Sci. USA* **103**, 3752–3757 (2006).
- Kuriyama, S. & Mayor, R. Molecular analysis of neural crest migration. *Phil. Trans. R. Soc. B* **363**, 1349–1362 (2008).
- Heaysman, J. E. Non-reciprocal contact inhibition. *Experientia* **26**, 1344–1345 (1970).
- Davis, E. M. & Trinkaus, J. P. Significance of cell-to-cell contacts for the directional movement of neural crest cells within a hydrated collagen lattice. *J. Embryol. Exp. Morphol.* **63**, 29–51 (1981).
- Dunn, G. A. & Paddock, S. W. Analysing the motile behaviour of cells: a general approach with special reference to pairs of cells in collision. *Phil. Trans. R. Soc. Lond. B* **299**, 147–157 (1982).
- Carney, T. J. *et al.* A direct role for Sox10 in specification of neural crest-derived sensory neurons. *Development* **133**, 4619–4630 (2006).
- De Calisto, J. *et al.* Essential role of non-canonical Wnt signalling in neural crest migration. *Development* **132**, 2587–2597 (2005).
- Matthews, H. *et al.* Directional migration of neural crest cells *in vivo* is regulated by Syndecan-4/Rac1 and non-canonical Wnt signaling/RhoA. *Development* **135**, 1771–1780 (2008).
- Tada, M. & Smith, J. C. *Xwnt11* is a target of *Xenopus* Brachyury: regulation of gastrulation movements via Dishevelled, but not through the canonical Wnt pathway. *Development* **127**, 2227–2238 (2000).
- Park, M. & Moon, R. T. The planar cell-polarity gene *stbm* regulates cell behaviour and cell fate in vertebrate embryos. *Nature Cell Biol.* **4**, 20–25 (2002).
- Carreira-Barbosa, F. *et al.* Prickle 1 regulates cell movements during gastrulation and neuronal migration in zebrafish. *Development* **130**, 4037–4046 (2003).
- Garriock, R. J., D'Agostino, S. L., Pilcher, K. C. & Krieg, P. A. Wnt11-R, a protein closely related to mammalian Wnt11, is required for heart morphogenesis in *Xenopus*. *Dev. Biol.* **279**, 179–192 (2005).
- Matthews, H., Broders-Bondon, F., Thiery, J. P. & Mayor, R. *Wnt11r* is required for cranial neural crest migration. *Dev. Dyn.* **237**, 3404–3409 (2008).
- Axelrod, J. D. *et al.* Differential recruitment of Dishevelled provides signaling specificity in the planar cell polarity and Wingless signaling pathways. *Genes Dev.* **12**, 2610–2622 (1998).
- Alfandari, D. *et al.* Integrin $\alpha 5 \beta 1$ supports the migration of *Xenopus* cranial neural crest on fibronectin. *Dev. Biol.* **260**, 449–464 (2003).
- Witzel, S. *et al.* Wnt11 controls cell contact persistence by local accumulation of Frizzled 7 at the plasma membrane. *J. Cell Biol.* **175**, 791–802 (2006).
- Condeelis, J., Singer, R. H. & Segall, J. E. The great escape: When cancer cells hijack the genes for chemotaxis and motility. *Annu. Rev. Cell Dev. Biol.* **21**, 695–718 (2005).
- Devreotes, P. N. & Zigmond, S. H. Chemotaxis in eukaryotic cells—a focus on leukocytes and *Dictyostelium*. *Annu. Rev. Cell Biol.* **4**, 649–686 (1988).
- Raz, E. Primordial germ-cell development: The zebrafish perspective. *Nature Rev. Genet.* **4**, 690–700 (2003).
- Keller, R. Cell migration during gastrulation. *Curr. Opin. Cell Biol.* **17**, 533–541 (2005).
- Lecaudey, V. & Gilmour, D. Organizing moving groups during morphogenesis. *Curr. Opin. Cell Biol.* **18**, 102–107 (2006).
- Risau, W. & Flamme, I. Vasculogenesis. *Annu. Rev. Cell Dev. Biol.* **11**, 73–91 (1995).
- Ayala, R., Shu, T. & Tsai, L. H. Trekking across the brain: the journey of neuronal migration. *Cell* **128**, 29–43 (2007).

Supplementary Information is linked to the online version of the paper at www.nature.com/nature.

Acknowledgements We thank M. Tada, M. Tawk, J. Clarke, C.-P. Heisenberg, R. Kelsh, L. Dale and S. Fraser for reagents, constructs and fish lines; C. F. Riaz for scanning electron microscopy images; and M. Bronner-Fraser, M. Raff, J. Green and A. Ridley for comments on the manuscript. This study was supported by grants to R.M. from the Medical Research Council (MRC) and the Biotechnology and Biological Sciences Research Council. H.K.M. and C.C.-F. are MRC and Boehringer Ingelheim Fonds PhD scholarship holders, respectively, and M.M. is an EMBO postdoctoral fellow.

Author Contributions C.C.-F. and R.M. designed the experiments. C.C.-F., H.K.M. and R.M. performed most of the experiments. C.C.-F. and R.M. did the movie analysis. C.C.-F., G.A.D. and R.M. planned and performed the statistical analysis. M.P., S.K., C.C.-F., H.K.M. and R.M. conducted the FRET analysis. M.M. made some of the constructs and the zebrafish transgenic. M.M., C.C.-F., H.K.M. and R.M. performed the PCP localization experiments. C.C.-F., C.S. and R.M. wrote the paper.

Author Information Reprints and permissions information is available at www.nature.com/reprints. Correspondence and requests for materials should be addressed to R.M. (r.mayor@ucl.ac.uk).